Journal of Power Sources 196 (2011) 5881–5888

Contents lists available at ScienceDirect

Journal of Power Sources

journal homepage: www.elsevier.com/locate/jpowsour

Proton exchange membrane fuel cell system diagnosis based on the signed directed graph method

Jianfeng Hua, Languang Lu, Minggao Ouyang*, Jianqiu Li, Liangfei Xu

State Key Laboratory of Automotive Safety and Energy, Tsinghua University, Beijing 100084, PR China

ARTICLE INFO

Article history:
Received 27 January 2011
Received in revised form 6 March 2011
Accepted 7 March 2011
Available online 11 March 2011

Keywords:
Proton exchange membrane fuel cell system
Signed directed graph diagnostic system
Qualitative and quantitative analysis
Signed directed graph model

ABSTRACT

The fuel-cell powered bus is becoming the favored choice for electric vehicles because of its extended driving range, zero emissions, and high energy conversion efficiency when compared with battery-operated electric vehicles. In China, a demonstration program for the fuel cell bus fleet operated at the Beijing Olympics in 2008 and the Shanghai Expo in 2010. It is necessary to develop comprehensive proton exchange membrane fuel cell (PEMFC) diagnostic tools to increase the reliability of these systems. It is especially critical for fuel-cell city buses serving large numbers of passengers using public transportation. This paper presents a diagnostic analysis and implementation study based on the signed directed graph (SDG) method for the fuel-cell system. This diagnostic system was successfully implemented in the fuel-cell bus fleet at the Shanghai Expo in 2010.

1. Introduction

The proton exchange membrane fuel-cell (PEMFC) hybrid bus is completely clean and environmentally friendly. It is regarded as an important alternative energy vehicle by the automotive industry and several governments. As a renewable energy resource, hydrogen can be produced from different kinds of energy sources, such as solar energy, bio-energy, electrical energy and other types of energy [1]. In July 2008 Beijing initiated a clean public transportation plan for the 29th Olympic Games. Fuel cell buses had operated on a specific bus line for one year as a green energy vehicle demonstration project for public transportation. For the 2010 Shanghai Expo, three fuel cell buses were brought into service to carry passengers between exposition halls. This clean, emission-free and low-noise bus was well received by the visitors from around the world. The State Key Lab of Automotive Safety and Energy at Tsinghua University started research on the fuel cell vehicle in 2002 and focused mainly on commercial vehicles [2]. The latest fuel cell bus fleet provided by Tsinghua University served at the 2010 Shanghai Expo as VIP reception buses (Fig. 1). The bus is powered by an AC motor with rated power of 150 kW plus 75 kW of braking energy regeneration. Two fuel cell stacks with a total rated power of 80 kW and a 80 Ah power battery are provided as the hybrid power source. The fuel cell and battery are separated by a DC–DC converter. Detail parameters for the vehicle and the power train are presented in Table 1.

Safety has been highlighted with the development of the modern automotive industry and has led to the mushrooming growth of fault diagnosis technology. The fault and incident rates in modern automotive systems, such as the fuel cell system, could result in increased casualties and loss of income, so fault diagnosis technology has been playing an increasingly important role in ensuring personal and equipment safety. From its beginning using basic experience, fault diagnosis technology has become an expert field relying on intelligent and integrated monitoring equipment and information technology. This has merged a large amount of electronic and computer technology. The importance of online fault diagnosis for the fuel cell hybrid electric bus is self-explanatory because of the high passenger numbers and long running times, as demonstrated over a year on a public transport route. The fuel cell system is a crucial part of the overall fuel cell hybrid system, because its satisfactory operation influences not only the safety of the whole bus, but also its cruising range. Hence, proper fault diagnosis of the fuel cell system during normal operating processes is necessary, because it not only ensures safety when the bus is running, but also protects the fuel cell system from severe damage under fault conditions.

Abbreviations: AC, alternating current; AFTCU, air flow and thermal control unit; AHCU, air humidification control unit; CAN, controller area network; CVM, cell voltage monitor; DC, direct current; DC/DC, direct current converter; FCU, fuel cell control unit; GSSEDM, generalized steady-state electro-chemical degradation model; GSSEM, generalized steady-state electro-chemical model; HSCU, hydrogen supply control unit; PEMFC, proton exchange membrane fuel cell; SDG, sign directed graph; SSEM, steady-state electro-chemical model; VCU, vehicle control unit.

* Corresponding author. Tel.: +86 10 62785706; fax: +86 10 62789699.
E-mail address: ouymg@tsinghua.edu.cn (M. Ouyang).

0378-7753/$ – see front matter © 2011 Elsevier B.V. All rights reserved.
doi:10.1016/j.jpowsour.2011.03.008

Nomenclature

A_{co}	heat-exchanger area of coolant (cm^2)
A_{fc}	activation area of fuel cell (cm^2)
C_a	specific heat capacity of air ($J\,kg^{-1}\,K^{-1}$)
C_{fc}	average specific heat capacity of the stack ($J\,kg^{-1}\,K^{-1}$)
C_{pa}	specific heat at constant pressure of air ($J\,kg^{-1}\,K^{-1}$)
C_{pw}	specific heat at constant pressure of the enthalpy wheel ($J\,kg^{-1}\,K^{-1}$)
C_{ra}	average specific heat capacity of radiator ($J\,kg^{-1}\,K^{-1}$)
D_W	humidity ratio of air on the adsorbent surface
E_0	open circuit voltage (V)
F	Faraday constant ($C\,mol^{-1}$)
F_V	core area and volumetric ratio of the enthalpy wheel
F_s	cross-sectional area ratio between the air flow and channel
h_{co}	convective heat transfer coefficient of coolant ($W\,m^{-2}\,K^{-1}$)
Δh_{vap}	enthalpy of formation when the reaction product is vapor ($J\,mol^{-1}$)
I_{fc}	fuel cell current output (A)
i	electric current in fuel cell empirical model (A)
i_{fc}	current density output of fuel cell ($A\,m^{-2}$)
J_{cp}	rotational inertia of compressor ($kg\,m^2$)
K_Y	mass transfer parameter
M_{cm}	rotational torque of air compressor (N m)
M_{cp}	load torque of air compressor (N m)
m	air flow per infinitesimal unit of cross section (kg)
m_{fc}	total mass of the stack (kg)
m_{N_2}	nitrogen mass of air intake (kg)
m_{O_2}	oxygen mass of air intake (kg)
m_{ra}	mass of radiator (kg)
N_{fc}	number of stack cell
N_{cvm}	channels of cell monitoring system
P_{air}	manifold pressure (kPa)
$P_{co,in}$	deionized coolant pressure (kPa)
P_H	hydrogen pressure (kPa)
$\dot{q}_{co}$	coolant heat transfer power (W)
$\dot{q}_{fc}$	thermal power of fuel cell (W)
R_1	cooling fan relay status (0-1)
R_U	main relay status (0-1)
R_H	hydrogen purge relay status (0-1)
T	stack operating temperature (°C)
$T_{ad,in}$	air temperature of enthalpy wheel inlet (°C)
$T_{ad,out}$	air temperature of enthalpy wheel outlet (°C)
$T_{ah,in}$	humidified air temperature of stack inlet (°C)
$T_{ah,out}$	air temperature of stack outlet (°C)
$T_{a,in}$	inlet air temperatures of radiator (°C)
$T_{a,out}$	outlet air temperatures of radiator (°C)
$T_{co,in}$	stack inlet temperature of deionized coolant (°C)
$T_{co,out}$	stack outlet temperature of deionized coolant (°C)
T_{fc}	average temperature inside the stack (°C)
T_{ra}	surface temperature of radiator (°C)
$T_{ra,in}$	coolant input temperatures of radiator (°C)
$T_{ra,out}$	coolant output temperatures of radiator (°C)
U_{fc}	total output voltage of the fuel cell system (V)
U_{fco}	main relay input voltage (V)
U_{sk1}	voltage of the first sub-module of the fuel cell stack (V)
U_{sk2}	voltage of the second sub-module of the fuel cell stack (V)
U_{sk3}	voltage of the third sub-module of the fuel cell stack (V)
U_{sk4}	voltage of the fourth sub-module of the fuel cell stack (V)
$V_{cvm,i}$	cell voltage of the i channel (V)
V_{fc}	cell voltage (V)
W_a	air flow ($kg\,s^{-1}$)
W_{co}	coolant flow ($kg\,s^{-1}$)
$W_{N_2,in}$	nitrogen flow of air intake ($kg\,s^{-1}$)
$W_{N_2,out}$	nitrogen flow of air exhaust ($kg\,s^{-1}$)
$W_{O_2,in}$	oxygen flow of air intake ($kg\,s^{-1}$)
$W_{O_2,out}$	remaining oxygen flow of air exhaust ($kg\,s^{-1}$)
$W_{O_2,rec}$	reacted oxygen flow ($kg\,s^{-1}$)

2. Diagnosis combining quantitative with qualitative analysis

There are two ways of applying fault diagnosis technology: one is based on modeling and the other is based on experimental data [3]. The method based on a modeling requires a systematic performance model to be built, and model changes to be analyzed, followed by fault testing and identification. The method based on data requires mathematical analysis of a large amount of historical process data to mine the information about the incident. However, such a system is already in industrial use, especially in some process industries. It is difficult to build precise quantitative models, but the mechanism influenced by processes and the relationships between elements in the system are clear. As a result, a new method based on qualitative model fault diagnosis is proposed using the mechanisms and relationships to build a qualitative model analysis system.

In the actual situation of fuel cell control and diagnosis, a complicated problem is the control system platform, such as microprocessors, cannot afford the large calculation when the vehicle needs a real time control to ensure the vehicle operation and safety, if the control algorithm is an all model-based process. The models of the fuel cell system and its components are mathematically too complicated to calculate in real time, especially the coupling of different models or multi-state description modeling. Therefore, the solution is using the large test data and empirical formulas to replace the large calculation in real time. The huge test data are organized as a lot of MAP tables, which are stored into the non-volatile memory of the fuel cell control system. The combination of qualitative reasoning with some specific techniques creates good

Fig. 1. A fuel cell city bus used at the 2010 Shanghai Expo.

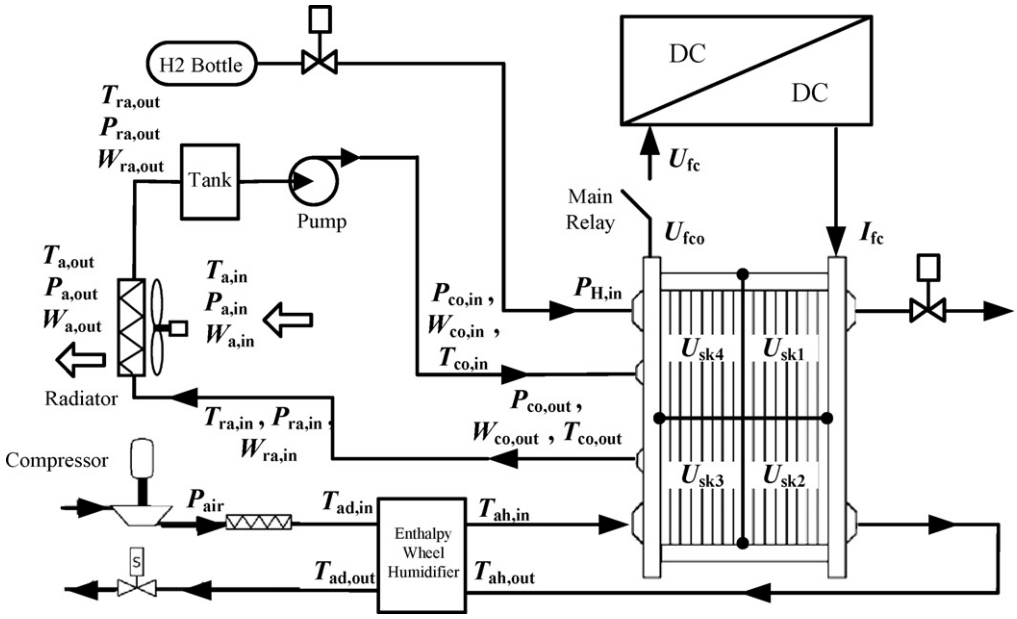

Fig. 2. Fuel cell system configuration scheme.

Table 1
Parameters of the fuel cell bus and the power train.

Parameter (unit)	Value
Vehicle mass (kg)	1.4672×10^4
Frontal area (m^2)	7.5
Drag coefficient	0.7
Rolling resistance coefficient	1.8×10^{-2}
Mechanical efficiency (%)	95
Mass factor	1.1
PEM fuel cell rated power (kW)	80
DC/DC rated power (kW)	80
Ni-MH battery rated capacity (Ah)	80
Electric motor peak power (kW)	150
Electric motor peak torque (N m)	1.121×10^3
Electric motor rated power (kW)	100
Electric motor maximal rotational speed (rpm)	6×10^3

opportunities for development, especially when using qualitative reasoning. The SDG (signed directed graph) model uses reasoning based on a qualitative model, but its reasoning methods can be divided into qualitative reasoning and semi-quantitative reasoning [4]. The main information used in qualitative reasoning is the SDG model and its samples, while semi-quantitative reasoning (or semi-qualitative reasoning) relies on further reasoning based on the SDG model and its samples by using quantitative information provided by the system. The processes and consequence of this tend to be a probability description or approximate description to express the possibility. The actual SDG model built was a qualitative, linear and initial responding model, while a lot of quantitative, nonlinear and transient information was not used when the model was built. If the information on model node and orientation is used, it will approach the semi-quantitative reasoning method. Fig. 2 presents the system structure of the fuel cell system following by models of each system, from which the corresponding SDG semi-qualitative model will be developed.

2.1. Stack model

When optimizing and controlling a fuel cell system, it is customary to describe the polarization characteristics of the stack by using empirical or semi-empirical models. The most classical semi-empirical model is Amphlett's SSEM (steady-state electro-chemical model) [5]:

$$\begin{cases} V_{fc} = E_0 + \eta_{act} + \eta_{ohm} \\ \eta_{act} = \xi_1 + \xi_2 T + \xi_3 T \ \ln(c^*_{O_2}) + \xi_4 T \ \ln(i) \\ \eta_{ohm} = -iR_{int} = -i(\xi_5 + \xi_6 T + \xi_7 i) \end{cases} \quad (1)$$

In the formula, E_0 is the open circuit voltage, i is the electric current, T is the stack operating temperature, $c^*_{O_2}$ is the oxygen concentration of catalyst layer, and ξ_{1-7} is the fitted parameter. Using this basis, Mann and Fowler addressed the GSSEM [6] (generalized steady-state electro-chemical model) and GSSEDM [7] (generalized steady-state electro-chemical degradation model) empirical models, respectively, by taking some factors into consideration, such as the ionic conductivity of the membrane changing with the change of water content of the membrane, and the lifespan of the cell, amongst others.

2.2. Hydrothermal system model

Theoretically speaking, the thermal power of a fuel cell can be obtained from the following formula [8]:

$$\dot{q}_{fc} = N_{fc} i_{fc} A_{fc} \left(-\frac{\Delta h_{vap}}{2F} - V_{fc} \right) \approx N_{fc} I_{fc} (1.25 - V_{fc}) \quad (2)$$

In the formula, $\dot{q}_{fc}$ is the thermal power of the fuel cell, N_{fc} is the number of each stack cell, i_{fc} is the current density output of the fuel cell, A_{fc} is the activation area of the fuel cell, Δh_{vap} is the enthalpy of formation when the reaction product is vapor, F is the Faraday constant, V_{fc} is the voltage of each cell, and I_{fc} is the current output from the fuel cell.

V_{fc} can be estimated using the measured values from the monitoring system for each fuel cell voltage. Assuming that N_{cvm} refers to the channels of each monitoring system, and $V_{cvm,i}$ refers to the voltage measured by the monitoring system in the i channel, can

be calculated from the following equation:

$$\hat{V}_{fc} = \frac{1}{N_{cvm}} \sum_{i=1}^{N_{cvm}} V_{cvm,i} \tag{3}$$

If a high degree of accuracy is not necessary, U_{fc} can be simply calculated with the output voltage of the fuel cell stack given as:

$$\hat{V}_{fc} = \frac{U_{fc}}{N_{fc}} \tag{4}$$

The heat absorbed by the coolant can be calculated using the following equation [9]:

$$\dot{q}_{co} = h_{co} A_{co} (T_{fc} - 0.5(T_{co,in} + T_{co,out})) \tag{5}$$

In the formula, $\dot{q}_{co}$ is the heat transfer power of the coolant, h_{co} is the convective heat transfer coefficient of the coolant, A_{co} is the heat-exchanger area, T_{fc} is the average temperature inside the fuel cell stack, and $T_{co,in}$ and $T_{co,out}$ are the input and output coolant temperatures of the stack, respectively. When the fuel cell heat exchanger surface is neglected, the heat transfer equation of the fuel cell stack can be represented as follows:

$$m_{fc} C_{fc} \frac{dT_{fc}}{dt} = \dot{q}_{fc} - \dot{q}_{co} \tag{6}$$

In the formula, m_{fc} is the total mass of the fuel cell stack, and C_{fc} is the average specific heat capacity of the fuel cell stack. Using the continuity equation for fluids, we can conclude that:

$$\begin{cases} W_{co,in} = W_{co,out} = W_{ra,in} = W_{ra,out} = W_{co} \\ W_{a,in} = W_{a,out} = W_a \end{cases} \tag{7}$$

The heat transfer equation of the radiator can be described as follows:

$$m_{ra} C_{ra} \frac{dT_{ra}}{dt} = W_{co} C_{co} (T_{ra,in} - T_{ra,out}) - W_a C_a (T_{a,out} - T_{a,in}) \tag{8}$$

In this equation, m_{ra} is the mass of the radiator, C_a is the specific heat capacity of air, C_{ra} is the average specific heat capacity of the radiator, T_{ra} is the surface temperature of the radiator, $T_{ra,in}$ and $T_{ra,out}$ are the input and output coolant temperatures of the radiator, respectively, W_a is the air flow, W_{co} is the coolant flow, and $T_{a,in}$ and $T_{a,out}$ are the air temperatures in and out of the radiator, respectively.

The flow through the cooling water pump is related to the rotational speed of the pump and the pressure difference through the pump. It can be shown that the flow through the pump is in direct proportion to the rotational speed, and the rotational speed depends on the control command. The relationship between the flow at a given rotational speed and the pressure difference can be shown by graph MAP, presented in Fig. 3.

2.3. Air system model

The air system model mainly includes the air compressor and enthalpy wheel humidifier models. The dynamic characteristics when the blower drives the machine can be presented as follows:

$$J_{cp} \frac{d\omega_{cp}}{dt} = M_{cm} - M_{cp} \tag{9}$$

In this equation, J_{cp} is the rotational inertia of the air compressor machine, ω_{cp} is the rotational speed of the air compressor machine, M_{cm} is the rotational torque of the air compressor, and M_{cp} is the load torque of the air compressor. According to the laws of conservation of mass and conservation of energy, we can obtain the following equations:

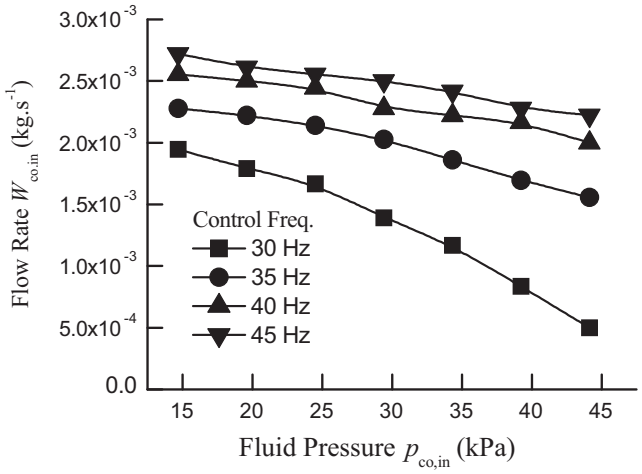

Fig. 3. Performance curves of the cooling water pump.

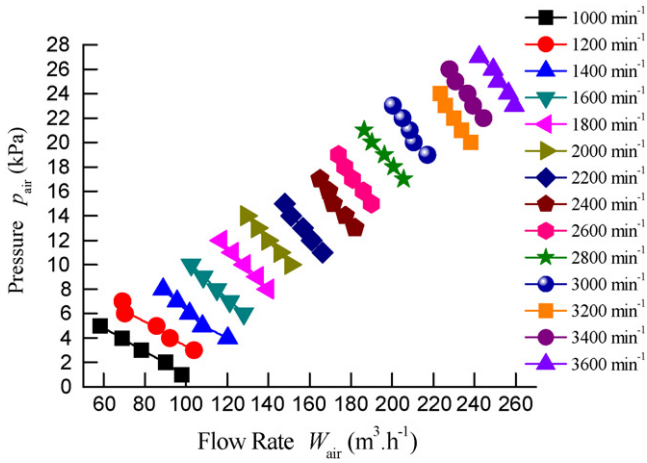

Fig. 4. Compressor performance curves.

$$\begin{cases} \frac{dm_{O_2}}{dt} = W_{O_2,in} - W_{O_2,out} - W_{O_2,rec} \\ \frac{dm_{N_2}}{dt} = W_{N_2,in} - W_{N_2,out} \end{cases} \tag{10}$$

In the equations above, m_{O_2} is the oxygen mass of air intake, m_{N_2} is the nitrogen mass of air intake, $W_{O_2,in}$ is the oxygen flow of air intake, $W_{O_2,out}$ is the remaining oxygen flow of air exhaust, $W_{O_2,rec}$ is the reacted oxygen flow, $W_{N_2,in}$ is the nitrogen flow of air intake, and $W_{N_2,out}$ is the nitrogen flow of air exhaust. When referring to the molar mass of oxygen, the following equation can be developed:

$$W_{O_2,rec} = M_{O_2} \frac{N_{fc} I_{fc}}{4F} \tag{11}$$

The performance characteristics under steady state conditions can be explained by graph MAP using experimental detection as shown in Fig. 4.

Fig. 5 is an illustration of the enthalpy wheel humidifier's theory, and shows that, in general, humidity is almost 100% when air is exhausted from the fuel cell stack. The enthalpy wheel absorbs heat and water from the air exhaust and stores them on the surface, after the air goes into the enthalpy wheel humidifier. When fresh air enters the enthalpy wheel humidifier, because the rela-

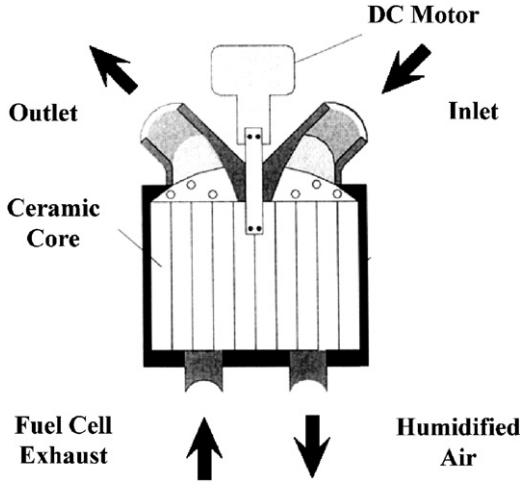

Fig. 5. Schematic diagram of the enthalpy wheel humidifier [11].

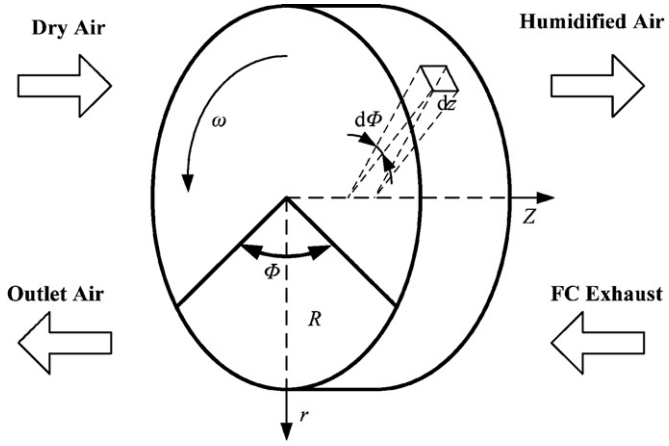

Fig. 6. Schematic diagram of the humidifying enthalpy wheel's construction.

tive humidity of fresh air is low, it will vaporize the water inside the enthalpy wheel and be led away to humidify the air intake. When the enthalpy wheel humidifier works at slow speed, the enthalpy wheel will, step by step, heat and humidify the fresh air and absorb heat and water from the air exhaust of the fuel cell, these being called the humidification process and the regenerative process of the enthalpy wheel, respectively. The core part of the enthalpy wheel humidifier is a honeycomb ceramic enthalpy wheel. This is a corrugated medium composition made of a special high temperature-resistant compound, often with cordierite as the main component [10].

An infinitesimal composition model of a humidifying enthalpy wheel can be built using the model building method for a desiccant wheel [12,13], and the mathematical model of the enthalpy wheel humidifier can then be obtained (Fig. 6).

Therefore, the mass conservation equation is:

$$\begin{cases} \dfrac{\partial D}{\partial t} + \omega \cdot \dfrac{\partial D}{\partial \phi} + \dfrac{m_i}{\rho_i F_s} \cdot \dfrac{\partial D}{\partial Z} = \dfrac{K_Y F_V}{\rho_i F_s} \cdot (D_W - D) \\ \dfrac{\partial W}{\partial t} + \omega \cdot \dfrac{\partial W}{\partial \phi} = \dfrac{K_Y F_V}{\rho_W F_V \delta_W} \cdot (D - D_W) \end{cases} \tag{12}$$

And the energy conservation equation is:

$$\begin{cases} \dfrac{\partial T}{\partial t} + \omega \cdot \dfrac{\partial T}{\partial \phi} + \dfrac{m_i}{\rho_i F_s} \cdot \dfrac{\partial T}{\partial Z} = \dfrac{\alpha F_V}{\rho_i F_s \cdot (C_{pa} + D \cdot C_{pv})} \cdot (T_W - T) \\ \dfrac{\partial T_W}{\partial t} + \omega \cdot \dfrac{\partial T_W}{\partial \phi} = \dfrac{\alpha F_V}{\rho_W F_V \delta_W \cdot (C_{pw} + W \cdot C_{ps})} \cdot (T - T_W) \\ \quad + \dfrac{K_Y F_V Q}{\rho_W F_V \delta_W \cdot (C_{pw} + W \cdot C_{ps})} \cdot (D - D_W) \end{cases} \tag{13}$$

In the equations above, i is the time coordinate, Z is the axial coordinate of the enthalpy wheel, ϕ is the circumference corner coordinate, D is the vapor portion of dry air in moist air, D_W is the humidity ratio of air on the adsorbent surface, m is the air flow per infinitesimal unit of cross section, F_V is the core area and volumetric ratio of the enthalpy wheel, F_s is the cross-sectional area ratio between the air flow and channel, C_{pa} is the specific heat at constant pressure of air, C_{pw} is the specific heat at constant pressure of the enthalpy wheel, W is the water absorption of the enthalpy wheel ceramic, α is the thermal conductivity between the enthalpy wheel ceramic core and air, K_Y is the mass transfer parameter, ρ_W is the adsorbent density, and δ_W is the depth of the adsorbent.

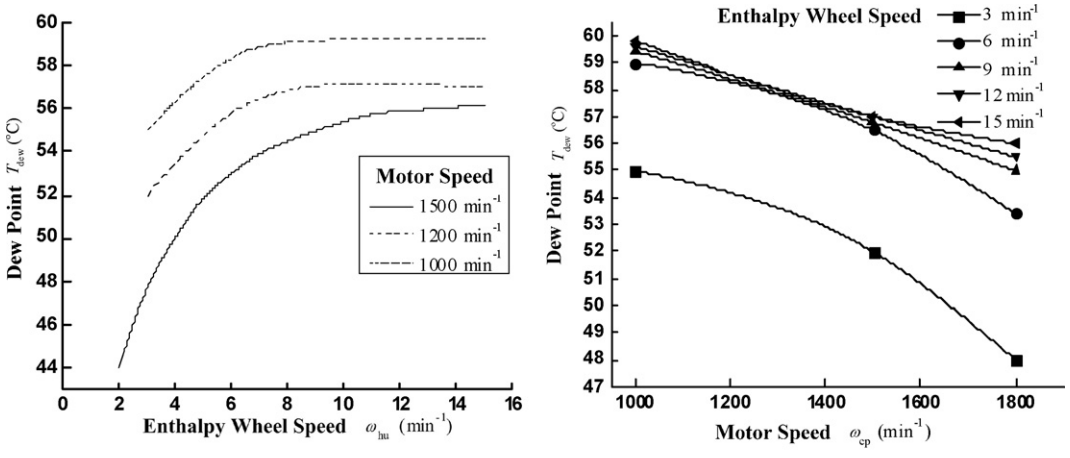

(a) relationship between humidification and speed of enthalpy wheel

(b) relationship between humidification of enthalpy wheel and speed of compressor

Fig. 7. Curves of humidification function of the enthalpy wheel during experiments.

Fig. 7 shows curve diagrams which describe the humidification function of the enthalpy wheel after experimental detection.

3. Fuel cell system SDG diagnosis model

Based on the definition of graph theory used in mathematics [14], and reference [15] we can obtain a rigorous mathematical expression of the SDG model:

$$G = (\boldsymbol{V}, \boldsymbol{E}, \varphi, \psi) \tag{14}$$

In the expression, the set of nodes $\boldsymbol{V} = \{v_1, v_2, \ldots, v_n\}$ represents the root of the system fault, spur track $\boldsymbol{E} = \{e_1, e_1, \ldots, e_m\}$ represents the 'cause influence' relationship between nodes, map $\varphi : \boldsymbol{E} \rightarrow \{+, -\}$ represents the positive and negative effects, map $\psi : \boldsymbol{V} \rightarrow \{+, 0, -\}$ represents the state of the nodes, $\varphi(e_k)$, $e_k \in \boldsymbol{E}$ represents the symbol of the spur track, $\psi(v_i)$, $v_i \in \boldsymbol{V}$ represents the symbol of the nodes. When the value of every node is defined, the symbol of the spur track $\varphi(e_k) \in \{+, -\}$ is given by the SDG model, and the symbol of the nodes $\psi(v_i) \in \{+, 0, -\}$ is given by the SDG model sample.

The process of building the SDG model is to ascertain the state of the nodes and spur tracks, and the way of building the mathematical model is to transfer quantitative mathematics into a qualitative SDG model. Therefore, every assembly is physically modeled and tested to get their qualitative relationships, and the symbol directional model of every system assembly is built by describing the causality between variables with the help of a graphical method, such as Fig. 8. This is the most basic SDG model, showing that there is a connection between the node variable A and the node variable B, while the symbol between the lines $\varphi : \boldsymbol{E} \rightarrow \{+, -\}$ refers to the relationship that may have a positive or negative effect, which can then be confirmed by models and practical experience.

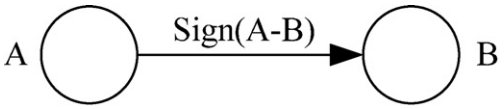

Fig. 8. Basic SDG model.

Fig. 9 represents the qualitative SDG model of the fuel cell system. In the graph, U_{fc} is the total output voltage of the fuel cell system, I_{fc} is the total output current of the fuel cell system, $T_{ah,in}$ is the humidified hot air temperature when the fuel cell stack is humidified by the enthalpy wheel, $T_{ah,out}$ is the temperature of the air in the stack after being humidified by the enthalpy wheel, $T_{ad,in}$ is the temperature of the air entering the humidifying enthalpy wheel from the exit of the blower, $T_{ad,out}$ is the temperature of the sweep gas from the humidifying enthalpy wheel when discharged into the atmosphere after dehumidifying, P_{air} is the manifold pressure, P_H is the hydrogen pressure, $P_{co,in}$ is the deionized coolant pressure, $T_{co,in}$ is the inlet temperature of the deionized coolant (relative stack), $T_{co,out}$ is the exit temperature of the deionized coolant (rel-

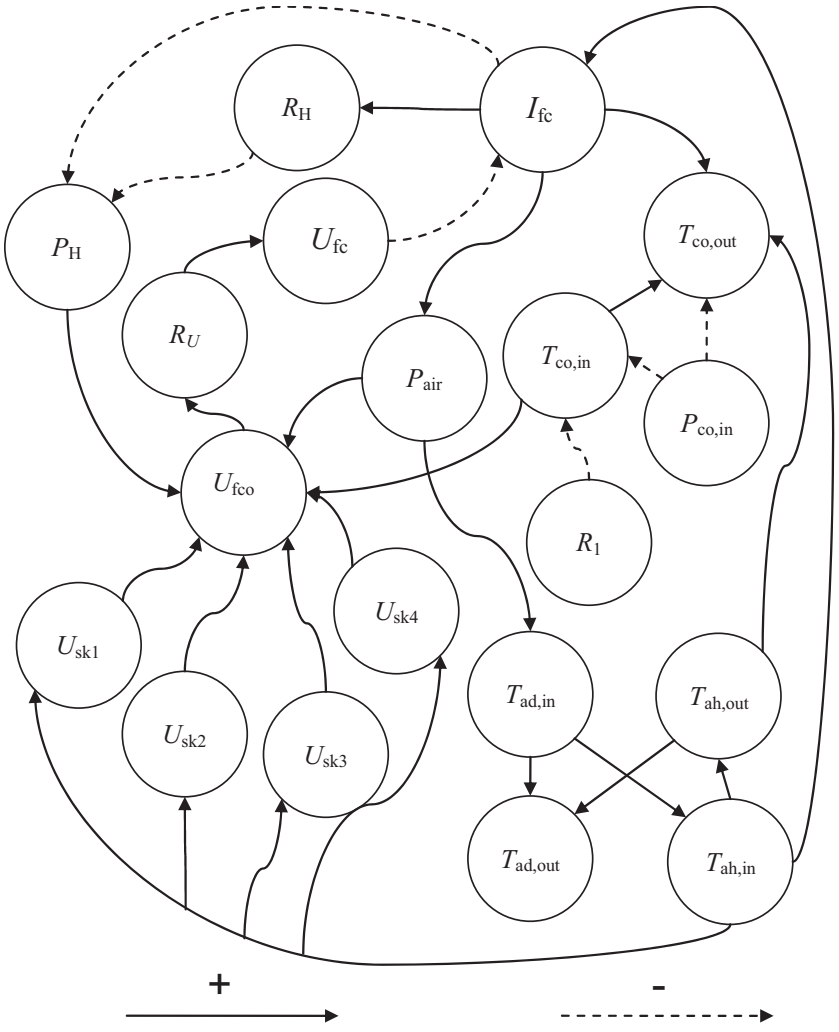

Fig. 9. Fuel cell system SDG model.

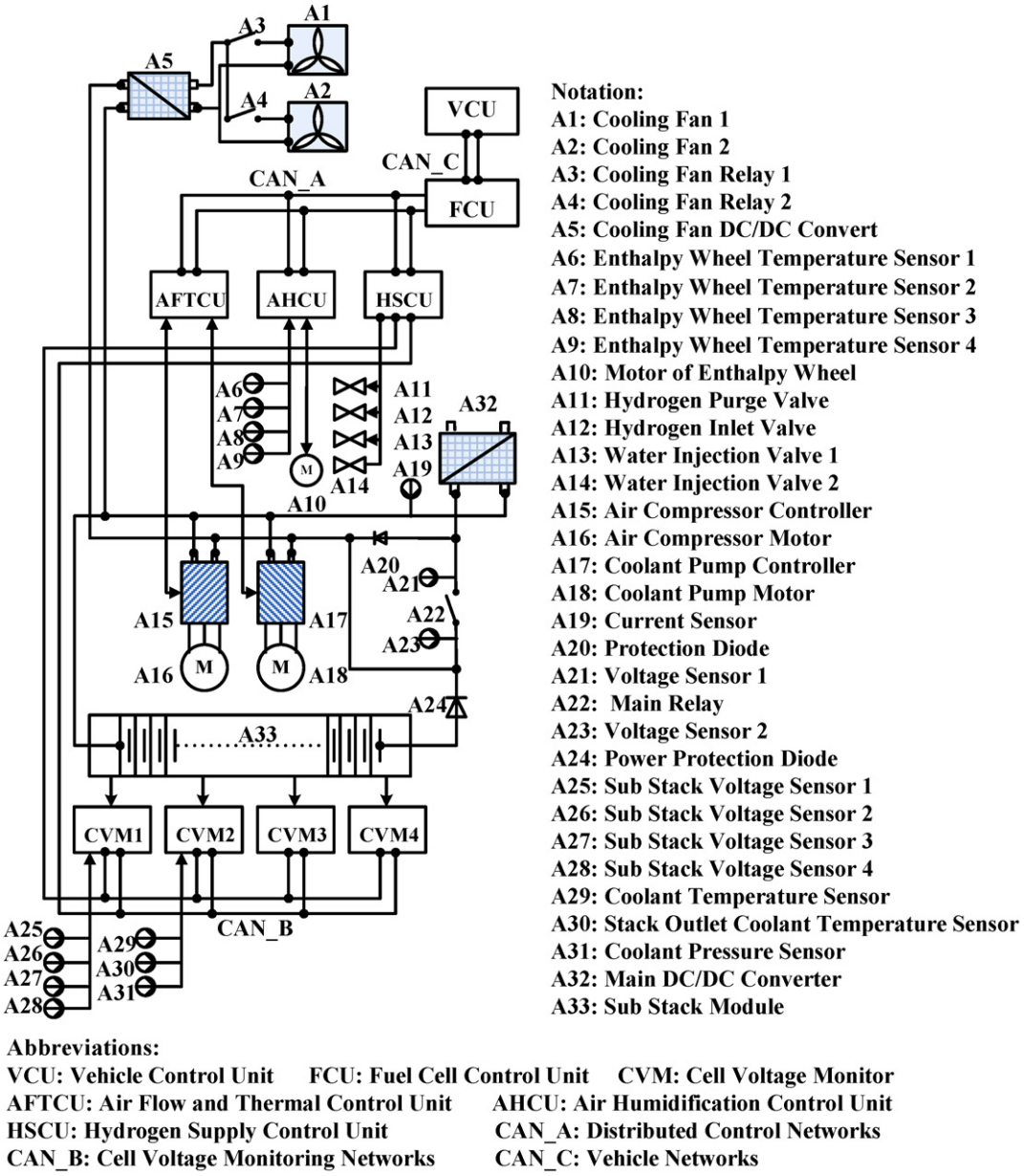

Fig. 10. Fuel cell control system and sensor networks.

ative stack), U_{sk1} is the voltage of the first sub-module of the fuel cell stack, U_{sk2} is the voltage of the second sub-module of the fuel cell stack, U_{sk3} is the voltage of the third sub-module of the fuel cell stack, U_{sk4} is the voltage of the fourth sub-module of the fuel cell stack, U_{fco} is the input voltage of the main relay, R_U is the main relay, R_1 is the cooling fan relay, and R_H is the hydrogen purge relay. The fuel cell control system and sensor networks, which acquire and monitor the sensor electronic signals to provide data flow for SDG model, are shown in Fig. 10.

According to the definition of SDG, there are three states in every state node: $\psi : \boldsymbol{V} \rightarrow \{+, 0, -\}$, where "+" means that the measured value of the state node is greater than the anticipated value, and similarly, "−" means smaller, and "0" means it is in the normal range. Valves R_1, R_U, R_H represent the operational state of the valve; where "+" means the state node cannot transfer a positive alteration of the measure value of the node's correlativity, and "−" means the node cannot transfer a negative alteration. Qualitative diagnosis based on rules can detect the occurrence of a system fault quickly to find the origin of the fault which can be obtained from the fault transmittal process in the SDG model.

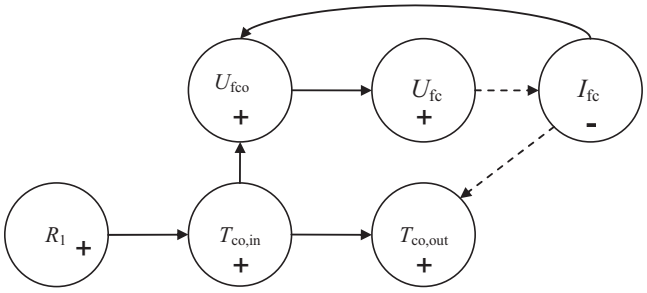

Fig. 11. The fault transmittal process of the cooling fan relay.

Fig. 11 represents a typical fault transmission process. Because of the damage to the cooling fan relay, the water temperature of the

Table 2
Fault transmittal process of the fuel cell system SDG method—the pump loses efficacy due to leakage.

Status	U_{fco}	U_{fc}	I_{fc}	P_{air}	$P_{co,in}$	P_H	$T_{co,in}$	$T_{co,out}$	$T_{ah,in}$	$T_{ad,in}$	$T_{ah,out}$	$T_{ad,out}$	R_1	R_U	R_H	U_{sk1}	U_{sk2}	U_{sk3}	U_{sk4}
1	0	0	0	0	0	0	0	0	0	0	0	0	0	0	0	0	0	0	0
2	0	0	0	0	–	0	0	0	0	0	0	0	0	0	0	0	0	0	0
3	0	0	0	0	–	0	+	+	0	0	0	0	0	0	0	0	0	0	0
4	0	0	0	0	–	0	+	+	+	0	+	+	0	0	0	0	0	0	0
5	+	+	–	0	–	0	+	+	+	0	+	+	0	0	0	+	+	+	+

Table 3
Fault transmittal process of the fuel cell system SDG method—blower loses efficacy from being blocked.

Status	U_{fco}	U_{fc}	I_{fc}	P_{air}	$P_{co,in}$	P_H	$T_{co,in}$	$T_{co,out}$	$T_{ah,in}$	$T_{ad,in}$	$T_{ah,out}$	$T_{ad,out}$	R_1	R_U	R_H	U_{sk1}	U_{sk2}	U_{sk3}	U_{sk4}
1	0	0	0	0	0	0	0	0	0	0	0	0	0	0	0	0	0	0	0
2	0	0	0	–	0	0	0	0	0	0	0	0	0	0	0	0	0	0	0
3	–	–	0	–	0	0	0	0	0	+	0	0	0	0	0	–	–	–	–
4	–	–	–	–	0	0	0	0	+	+	0	0	0	0	0	–	–	–	–

Table 4
Fault transmittal process of the fuel cell system SDG method—hydrogen purge value is invalid.

Status	U_{fco}	U_{fc}	I_{fc}	P_{air}	$P_{co,in}$	P_H	$T_{co,in}$	$T_{co,out}$	$T_{ah,in}$	$T_{ad,in}$	$T_{ah,out}$	$T_{ad,out}$	R_1	R_U	R_H	U_{sk1}	U_{sk2}	U_{sk3}	U_{sk4}
1	0	0	0	0	0	0	0	0	0	0	0	0	0	0	+	0	0	0	0
2	–	–	0	0	0	0	0	0	0	0	–	0	0	0	+	–	–	0	0
3	–	–	–	0	0	0	0	0	0	0	–	0	0	0	+	–	–	–	–

fuel cell stack inlet rises abnormally, which may increase the water temperature near the exit. With the rising temperature, the activity of fuel cell stack increases and the voltage rises, so the output current flow decreases, as does the output power. However, because the fault can be isolated at the start, it seldom reaches such a state. Usually, when $T_{co,in}$ exceeds the threshold value, the control system will detect the abnormal state of the system and initiate safety measures or stop the engine, and then confirm or estimate the fault cause by comparing the fault transmittal processes. However, the comparison does not occur in real time when the bus is running, as in most cases, so the fault will be alarmed and the bus will stop running to guarantee the safety of the fuel cell system and allow the fault diagnosis process to finish.

Tables 2–4 show the fault transmittal processes for different SDG models.

4. Conclusion

To achieve the commercialization of fuel cell vehicles, several obstacles need to be overcome before fuel cell vehicles appear on the market at a commercial price. One of these is the development of a powerful diagnostic system to increase the reliability of fuel cell power systems because of the potential dangers of hydrogen. In this paper, a new fault diagnosis methodology, based on the SDG method, has been presented and implemented in the fuel cell systems for shuttle buses at the 2010 Shanghai Expo. An advantage of this new methodology is that it does not require accurate modeling and a powerful computing capability to provide a diagnosis. This can be carried out by the in-vehicle control system and the fuel cell control system during road use. The SDG based diagnostic method and overall diagnosis protocol were established during the public demonstration of the fuel cell bus at the 2010 Shanghai Expo. Any system failures and component degradation could be easily detected and observed using these methods.

Acknowledgments

This work is part of the project on "Research and Development of the Fuel Cell City Bus" in China. The authors appreciate the financial support provided by the National 863 Hi-tech Research Program during the 11th five-year plan of China.

References

[1] L. Frisch, PEMFC Stack Sealing Using Silicone Elastomers, SAE Paper 2003-01-0801.
[2] Y. Jia, H. Wang, M. Ouyang, Journal of Power Sources 155 (2006) 319–324.
[3] V. Venkat, R. Rgahunathna, Y. Kewen, et al., Computers and Chemical Engineering 27 (3) (2003) 293–311.
[4] M. Liu, Research and Application of Diagnosis based on SDG Modeling, Tsinghua University, Beijing, 2005 (dissertation).
[5] J.C. Amphlett, R.M. Baumert, R.F. Mann, et al., Journal of the Electrochemical Society 142 (1) (1995) 1–8.
[6] R.F. Mann, J.C. Amphlett, M.A.I. Hooper, et al., Journal of Power Sources 86 (1–2) (2000) 173–180.
[7] M.W. Fowler, R.F. Mann, J.C. Amphlett, et al., Journal of Power Sources 106 (1–2) (2002) 274–283.
[8] J. Larminie, A. Dicks, Fuel Cell Systems Explained, John Wiley & Sons, 2003.
[9] Y. Zhang, M. Ouyang, Q. Lu, et al., Applied Thermal Engineering 24 (2004) 501–513.
[10] Z. Lu, S. Xu, H. Ni, Vehicle Engine 173 (1) (2008) 50–53.
[11] S. Xu, X. Cheng, B. Li, Automotive Technologies 3 (2006) 18–21.
[12] P. Li, Z. Qiu, J. Shen, Journal of Tongji University (Natural Science) 32 (3) (2004) 327–331.
[13] H. Hao, Y. Zhang, J. Lu, et al., Heating Ventilating & Air Conditioning 35 (12) (2005) 57–61.
[14] J.A. Bondy, U.S.R. Murty, Graph Theory with Applications, Elsevier Science Publishing Co. Inc., New York, 1976.
[15] T. Umeda, T. Kuriyama, H. Matsuyam, et al., Chemical Engineering Science 35 (12) (1980) 2379–2388.